UDC 621 . 791 . 763 . 1 : 621 .791 . 72 : 629 . 11 . 011 . 5

Technical Report

Current Problems and the Answer Techniques in Welding Technique of Auto Bodies — First Part

Seiji FURUSAKO*
Gen MURAYAMA
Hatsuhiko OIKAWA
Tetsuro NOSE
Fuminori WATANABE
Hideki HAMATANI
Yasuo TAKAHASHI

Abstract

Application of high strength steel for the auto body has been increasing, because lightness is required in order to reduce CO_2 emissions at the same time as the high collision safety. This paper focused on technology trend and research progress concerning welding techniques which are being used for the assembly of auto bodies. On the resistance spot welding, the following results were introduced: 1) stress analysis by FEM in case of cross tension test for joint using high strength steel sheet, 2) improvement technique of cross tension strength based upon the FEM analysis, 3) welding technique of three steel sheets with a combination of substantially different thicknesses and 4) welding tecnique of an open section component like a hydroformed one.

1. Introduction

It is said that resistance spot welding was first used to weld frying pan handles around 1900. By 1946, the year following the end of World War II, this welding method had begun to be applied in the fabrication of car bodies.[1)] As increasing amounts of automotive steel sheet of higher strength have been used in recent years, the inferior cross-tension strength (CTS) of high-strength steel joints has been highlighted. Using steel sheet of higher strength is essential to reduce the weight of car bodies and secure the required levels of crashworthiness. Conversely, inferior CTS can frustrate the adoption of steel sheet of higher strength. Therefore, we investigated why the CTS of high-strength steel joints is low from the standpoint of fracture mechanics; on the basis of our results, we attempted to develop a new welding technique to enhance CTS.

Incidentally, the demand for lighter car bodies has necessitated a reduction in the thickness of automotive panels. Today, even steel sheets as thin as 0.55 mm are used for such panels. Consequently, when welding three sheets that differ significantly in thickness with a thin sheet set adjacent to the electrode, it is not always possible to form a nugget at the interface between the thin sheet and any of the thick sheets. Conversely, in spot welding (a point-joining method), the backlash between welding points causes member stiffness to decrease. In order to enhance the stiffness, it is expected that hydroforming (which allows solid structures with closed cross sections to be obtained) will be applied. However, the electrode sinks during the welding operation when an attempt is made to spot weld a steel sheet to a hollow member; this makes it impossible to obtain the welding current density required to form a desired nugget. This report also describes the results of the latest research into welding methods for parts to which spot welding can hardly be applied.

2. Spot Welding

2.1 Strength of spot-welded joints of high-strength steel sheets

The use of high-strength steels (tensile strength of at least 590 MPa) has been expanding in an effort to meet the safety standards

* Senior Researcher, Welding & Joining Research Center, Steel Research Laboratories
20-1 Shintomi, Futtsu, Chiba 293-8511

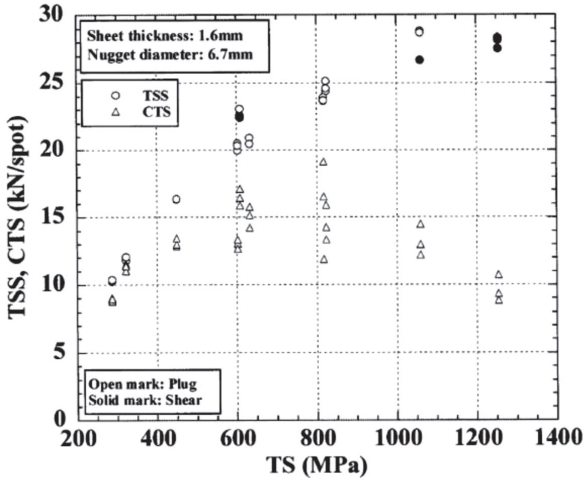

Fig. 1 Effect of tensile strength of steel sheet on TSS and CTS of spot welded joints

of car bodies and reduce environmental impacts (that is, to enhance the crashworthiness of car bodies and reduce their weight simultaneously). Presently, some steel sheets have tensile strengths of 1,500 MPa or more. Such steels are subjected primarily to hot press forming.[2] The strengths of spot-welded joints are illustrated in **Fig. 1**. The tensile shear strength of welded joints tends to increase with increasing steel sheet strength. Conversely, the CTS of welded joints tends to decline when the steel sheet strength is 780 MPa or more.[3] This is thought to occur for the following reason. With increasing steel sheet strength, the stress concentration at the nugget edge increases,[4] and nugget ductility and toughness decrease. When the amount of any added element (such as C) is increased in order to secure the desired steel sheet strength, the hardness of the weld metal (nugget) obtained increases; this, in turn, causes the nugget toughness to decrease. Nugget toughness also decreases when the contents of embrittling elements (P and S) are increased. The following equation of equivalent carbon content has been proposed to express the effects of these elements has been known.[5]

$$Ceq\ (spot) = C + Si/30 + Mn/20 + 2P + 4S \leqq 0.24\ (\%)$$

It is believed that C, Si, and Mn contribute to the increase in nugget hardness and P and S contribute to the increase in segregation, thereby causing a decline in nugget toughness. The threshold value on the right hand side represents the strength of a welded joint and the soundness of the fracture mode in a cross-tension test. When Ceq (spot) is within the range indicated by the above equation, fractures always occur outside the nugget (plug fracture) and CTS is high. However, attempts have been made to enhance CTS by controlling the composition of steel sheet appropriately. Sakuma et al. reported that even when the steel sheet strength is maintained constant, the strength of the weld increases as C content decreases and Si content increases.[6] This is thought to occur for the following reason. With the increase in C content, the hardness of the weld increases and the sensitivity of the fracture to the stress concentration at the nugget end increases, thereby causing CTS to decline. By contrast, as the content of Si—a hardenability element—is increased, the region that is quench-hardened by Si widens, that is, the change in hardness in the region from the nugget to the base metal becomes milder, thereby improving CTS.

2.2 Fracture analysis in cross-tension test

According to a well-known material mechanics model, it is expected that the CTS of the spot welded joints will improve with the increase in steel sheet strength. However, this contradicts the observed phenomenon (Fig. 1). Therefore, we considered a cross-tension test[7] based on fracture mechanics and attempted to clarify the dominant factors of CTS.

Understanding the fracture of spot-welded joints in the cross-tension test as a problem of crack propagation from around the nugget, we studied the problem using an elastic-plastic fracture mechanics model in order to obtain a general understanding of fractures, from the ductile fracture to the brittle fracture. According to elastic-plastic fracture mechanics, it is assumed that the crack starts to propagate when the crack propagation driving force (J) around the nugget under a tensile load reaches the fracture toughness (J_C) of the nugget edge. Therefore, we attempted to derive the value of J and measure the value of J_C of the edge during the cross-tension test.

In order to derive the value of J, we applied an additional method in the cross-tension test to calculate the value of J from the change in potential energy caused by virtual crack propagation in an elastic-plastic FEM analysis.[8] In the cross-tension test of a spot-welded joint, the test piece (which has been prepared by putting one steel sheet over another in a cross shape and welding them at the center point) is subjected to the load that causes the steel sheets to separate. Therefore, the stress that is applied to the nugget increases not axisymmetrically, but at four points 90° apart in the same plane. We decided to let the virtual cracks propagate from one of these points. In the FEM analysis, a half-scale model that considered the symmetry of the joint was prepared. The above method was used to evaluate the dependence of the J-value on nugget diameter and crack propagation direction. Three levels of nugget diameter, based on the square root of sheet thickness t (= 1.2 mm), were considered: $3\sqrt{t}$, $4\sqrt{t}$, and $5\sqrt{t}$. In addition, we modeled virtual cracking in the interfacial direction (parallel to the sheet surface) and the thickness direction, corresponding to the initial crack propagation in the nugget fracture and the plug fracture, respectively.

Fig. 2 shows the distribution of maximum principal stress at the nugget edge under a load of 4 kN. The broken line in the figure indicates the fusion line. It is clear that the virtual crack in the edge opened during the deformation. The decline in potential energy caused by the opening was divided by the crack area to obtain the value of J. **Fig. 3** shows the dependence of the J-value on nugget diameter under a load of 5 kN, obtained for each of the two types of cracks. It is clear that, in either cracking direction, the J-value under the same load decreases with the increase in nugget diameter. According to the analysis result obtained for a nugget diameter of $3\sqrt{t}$, the J-value when the crack was allowed to propagate in the interfacial direction was slightly larger than that when the crack was allowed to propagate in the sheet thickness direction. However, for larger nugget diameters ($4\sqrt{t}$ and $5\sqrt{t}$), the J-value when the crack was allowed to propagate in the sheet thickness direction became larger than that when the crack was allowed to propagate in the interfacial direction.

The above analysis results agree with the experimental results, indicating that CTS increases and the fracture mode of fracture changes from a nugget fracture to a plug fracture with an increase in nugget diameter. This confirms that the concept of J-value in FEM analysis is useful in FEM analysis in a cross-tension test. Therefore, we believe it is possible to improve CTS by restraining the increase in the J-value or increasing the fracture toughness, J_C, of the edge.

Incidentally, no authors have yet reported the local J_C that serves as a criterion for the propagation of cracks in a spot weld. Therefore,

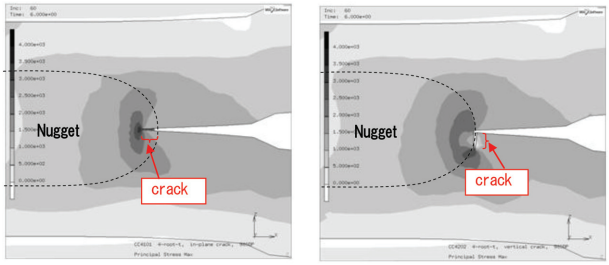

Fig. 2 Deformed state and distribution of maximum principal stress at edge of nugget under the load of 4kN

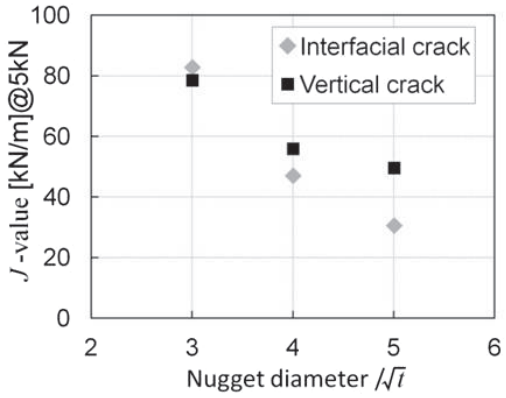

Fig. 3 Dependence of J-value on nugget diameter under the load of 5kN

we used the scale compact tension (CT) specimens to measure the edge J_C of two types of 980 MPa steel sheets with different composition systems. In addition, we measured the CTS of each of the spot-welded joints of the two steel sheets and compared the measured CTS with the measured J_C. Furthermore, we compared the morphology of fracture surface between the two types of specimens.

The specimens used were a 0.13% C steel sheet and a 0.30% C steel sheet (thickness: 1.4 mm), both of 980 MPa class; spot-welded joints of steel sheets of the same type (nugget diameter: $4\sqrt{t}$) were prepared. The welding machine used was a servomotor-driven, single-phase, AC, stationary spot welder. The AC frequency was 50 Hz (the same applies in the sections that follow), with 1 cycle being 20 ms. Using a welding force of 3.4 kN and welding time of 16 cycles, $4\sqrt{t}$ nuggets were formed by adjusting the current value.

As shown in **Figs. 4 and 5**, a 1:25-scale specimen (thickness B = 1 mm, width W = 2 mm) of inch-sized CT specimen was cut out from the end of each of the joint nuggets prepared. A pressure-welded part (corona bond), which peels off under a small load, was used as the precrack. The crack opening load was applied by pulling a wire that was passed through a hole in the test piece and attached to the tensile test machine at a rate of 200 μm/min. Under the assumption that K_Q (derived from the specimen breaking load in accordance with JIS G 0564) was equal to the fracture toughness value, K_C, the value of K_C was calculated to be 84 MPam$^{1/2}$ or more for the 0.13% C nuggets and 29 MPam$^{1/2}$ for the 0.30% C nuggets. The values of J_C obtained by conversion from the values of K_C were estimated to be 30 kN/m or more and 3.7 kN/m or more, respectively. As shown in **Fig. 6**, the fractured 0.30% C specimen revealed a grain boundary fracture at the edge and a cleavage fracture surface inside the nugget.

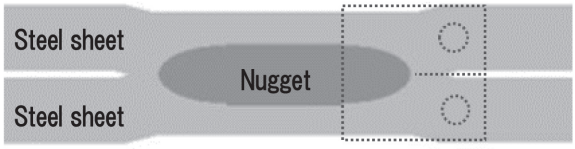

Fig. 4 Specimen preparation position

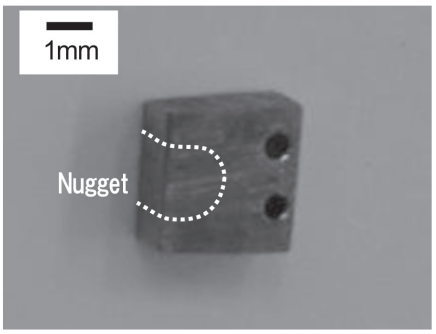

Fig. 5 Appearance of miniature CT specimen

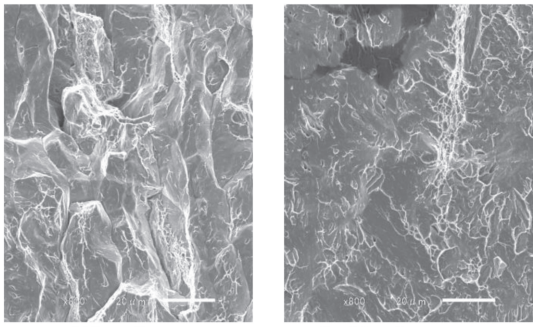

Fig. 6 SEM images of fracture surface of miniature CT specimen after testing (0.30mass%C)

The CTS of welded joints was 2.4 kN for the 0.30% C steel sheet and 6.6 kN for the 0.13% C steel sheet, the ratio between them being 0.38. According to the fracture toughness test results, the fracture stress ratio ($[J_C$ (0.30%C) / J_C (0.13%C)$]^{1/2}$; the square root of J is proportional to stress) is 0.35. Thus, the above ratio was close to the test result. The 0.30% C joint subjected to the cross-tension test revealed a grain boundary fracture at the edge and a cleavage fracture surface inside the nugget.

As described above, comparison between the results of fracture toughness and cross-tension tests using miniature CT specimens verified that the CTS of welds with low fracture toughness (J_C) tends to be low and that the modes of fracture observed in both tests are the same. Therefore, it is considered that similar fracture phenomena occurred in the above tests, suggesting the possibility that CTS should be governed by the fracture toughness of the edge. It can be expected, therefore, that CTS will improve when the fracture toughness (J_C) of the edge is increased.

2.3 Improvement in CTS by post-heat conduction

As described in Section 2.1, the joint strength in the peeling direction begins to decrease when the base metal strength exceeds 780 MPa. With this in mind, Hamatani et al. studied post-heat conduc-

tion—the process whereby conduction occurs after a short cooling time at the end of regular conduction. They found that the CTS of high-strength steel joints could be improved by using appropriate conditions for post-heat conduction.[9] Unlike the conventional tempering process in which the weld is tempered after a sufficient cooling time (i.e., after completion of martensite transformation of the weld), the post-heat conduction process incorporates a short cooling time; hence, it will not cause significant decline in productivity. The post-heat conduction process is described in detail below.

The material used was a 2-mm-thick aluminized hot-stamped steel sheet. The test piece shape was the same as that for a cross-tension test specified in JIS Z 3137. A single-phase AC spot welder of stationary type was used as the welding machine. The welding force was maintained at 5 kN. The welding current was passed in two discrete steps—the regular conduction for forming nuggets and the post-heat conduction for reforming them. A cooling time during which the welding current was not passed was provided between the regular conduction and post-heat conduction, and the cooling time was varied in the test. In a preliminary test, it was decided to use a welding current (I_1) of 8.2 kA and a conduction time of 19 cycles (AC power frequency: 50 Hz) so that a nugget diameter of $5\sqrt{t}$ (t: sheet thickness) could be obtained during the regular conduction.

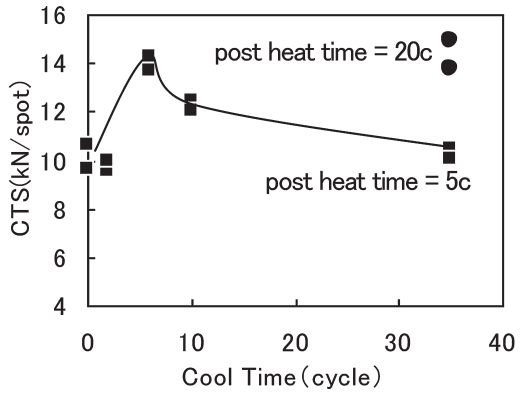

Fig. 7 Effect of cool time on CTS (HS, sheet thickness 2.0mm, nugget diameter $5\sqrt{t}$)

Additionally, in another preliminary test, the welding current (I_2) during the post-heat conduction was set at 90% of I_1 and the post-heat conduction time was set at 5 or 20 cycles.

Fig. 7 illustrates the effect of cooling time on CTS. It is clear that CTS reaches a peak for a cooling time of 6 cycles and improves when the post-heat conduction time is increased, even when the cooling time is increased to 35 cycles. With the aim of investigating why CTS improved, as described above, we analyzed the conditions of solidification segregation at the edge of the nugget using a field emission electron probe microanalyzer. The analysis revealed segregations of, for example, Mn, Si, and P. An example of P segregation is shown in **Fig. 8**. When post-heat conduction was not performed at all or was performed using the conditions under which CTS did not improve (as shown in Fig. 8 (a)), the solidification-segregated P was found to remain in the nugget. Conversely, with a cooling time of 6 cycles (which improved CTS, as shown in Fig. 8 (b)), the segregation of P in the same part decreased markedly. One reason for this is thought to be as follows. The element that was solidification-segregated during regular conduction was diffused during the post-heat conduction. As described in the preceding section, it is believed that the toughness of the nugget edge increased, thereby helping to enhance CTS.

The effect of post-heat conduction in easing such solidification segregation is supported by the results of Taniguchi et al.[10] It should be noted that the hardness of the nugget interior remains the same, regardless of whether the post-heat conduction is implemented. Therefore, the above improvement in CTS cannot be attributed to the effect of tempering. Conversely, the application of post-heat conduction increased the degree and width of softening of the heat-affected zone (HAZ). From the standpoint of fracture mechanics, the degree of influence of the widening of soft HAZ on the improvement in CTS was estimated to be about 4%.[11] Therefore, the improvement in CTS by post-heat conduction can be attributed mainly to the enhancement of fracture toughness by the easing of solidification segregation.

2.4 Spot welding of three steel sheets with large thickness ratio

Car parts such as side panels are fabricated by spot welding three steel sheets together. When the outer steel sheet is a thin sheet

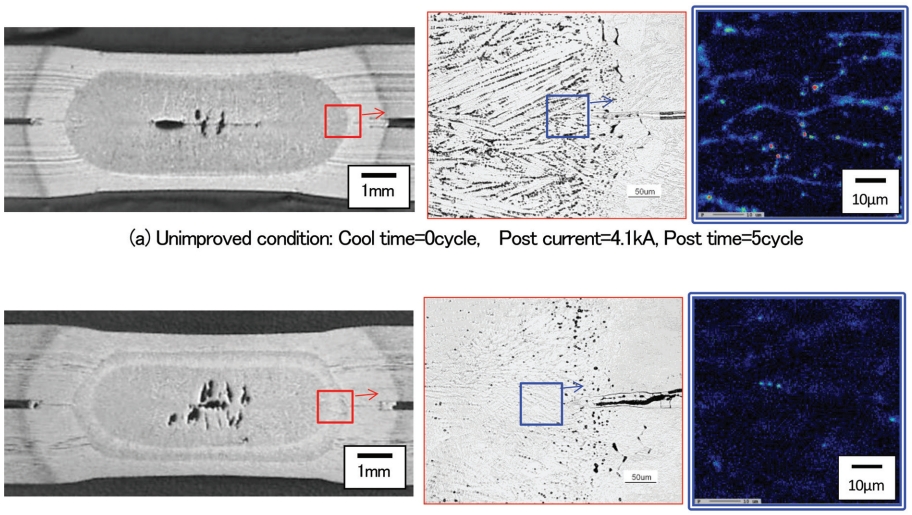

Fig. 8 Effect of post heat condition on micro-structure and solidification segregation at edge of nugget

of mild steel and the reinforcement steel sheets are thick sheets of high strength steel (that is, when there is a large thickness ratio between the sheets), it is often difficult to spot weld such sheets together.[12] The term "thickness ratio" as used herein refers to the total thickness of the three steel sheets divided by the thickness of the thinnest steel sheet. Nuggets obtained by spot welding of three steel sheets are illustrated in **Fig. 9** (a). In the spot welding of three steel sheets with a large thickness ratio, it is difficult to form a nugget at the interface between thin and thick steel sheets, as shown in Fig. 9 (b). The reason for this is that in spot welding, because of heat removal by the water-cooled electrode, the fusion progresses from the thickness center of the three steel sheets toward the outside, with the exception of the heat generated by contact resistance at the steel sheet surfaces in the early stages of welding time. In addition, in view of the dimensional accuracies of actual members, it is necessary to set appropriate welding conditions when there is a gap between steel sheets. In practice, the proper welding current range is as shown in **Fig. 10**. However, the welding current range is often narrower in one-step spot welding.

As a means of solving the above problem when there is no gap between the steel sheets, a method has been proposed in which the diameter of the electrode tip at the thin-sheet side is reduced and the

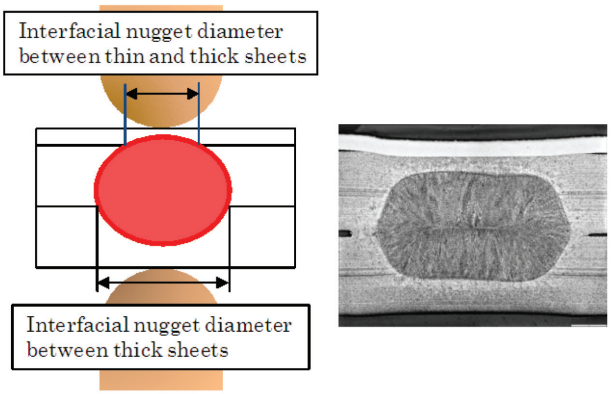

(a) Definition of nugget dia. (b) Cross section of spot-weld

Fig. 9 Three sheets spot-welding

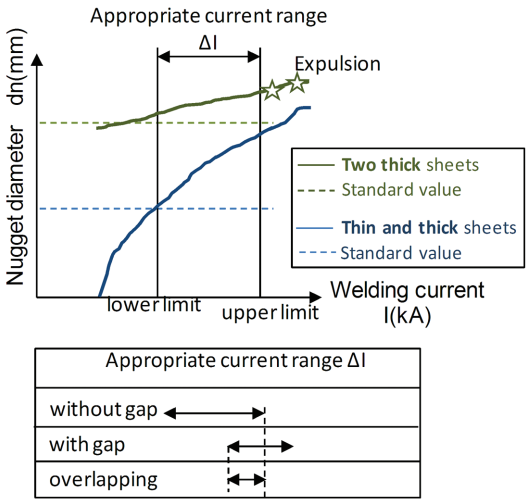

Fig. 10 Weldability lobe of three sheets spot-welding

welding force and current are varied during the welding time.[13] In addition, a two-step pulsating current welding method (**Fig. 11**) has been proposed in which neither the electrode diameter nor the welding force are changed.[14] This method is described briefly below. Initially, during the first welding step, a relatively large welding current is passed to generate heat by utilizing the contact resistance at the interface between the thin and thick steel sheets. Next, during the second welding step, a small welding current is passed in a pulsating manner to ensure stable growth of nuggets at both the interface between the thin and thick steel sheets and that between the thick steel sheets. This method does not positively utilize the contact resistance that is effective when the electrode force is low. Since the method can be applied even under a high electrode force, it is particularly effective when there is a gap between the steel sheets to be welded together.

An experiment was conducted by using the above technology. The materials used were a 0.6-mm-thick sheet of mild steel and two 1.6-mm-thick sheets of high-strength steel (980 MPa class). Spacers 1.4 mm in thickness were inserted at intervals of 40 mm between the thin and thick steel sheets and between the thick steel sheets. A servomotor-driven, single-phase AC welder was used for the test. The electrode used was a chromium-copper dome radius type with a tip radius of 40 mm and tip diameter of 6 mm. The welding force was 3.43 kN. In order to evaluate the diameter of fusion at the interface between the thin and thick sheets, which determines the proper current range, we conducted a chisel test at the interface and evaluated the plug diameter.

The test results are illustrated in **Fig. 12**. The horizontal axis represents the first-step welding current for one-step welding (welding

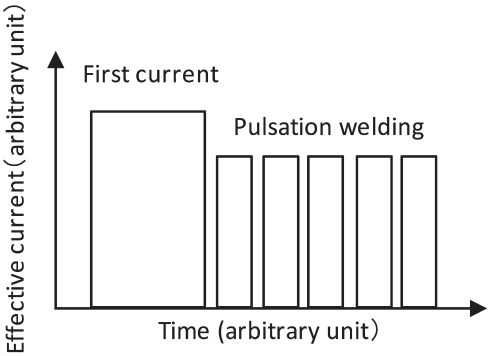

Fig. 11 Image of welding current pattern

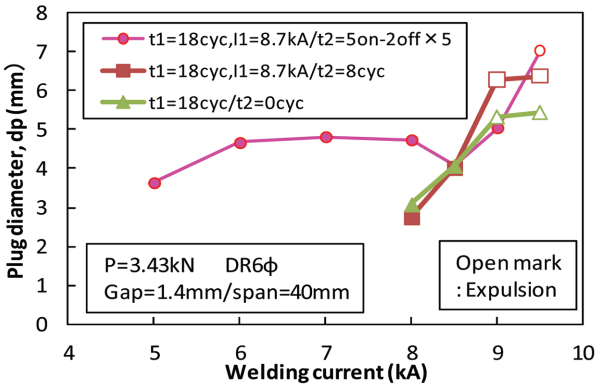

Fig. 12 Weldability lobes by different welding current patterns

time t_1 = 18 cycles) and the second-step welding current for two-step welding (first welding time t_1 = 18 cycles, second welding time t_2 = 8 cycles) or pulsation welding (t_1 = 18 cycles, t_2 = (5 cycle heat-2 cycle cool) × 5). For one-step or two-step welding, the welding current range was less than 1 kA. Conversely, with pulsation, it was possible to secure a proper welding range of 3 kA or more (about 1.8 kA when there was no gap between the steel sheets).

2.5 Application of spot welding to hollow members

In spot welding of car bodies, the so-called direct spot welding (in which the welding current is passed while two or more steel sheets are pressed against each other) by the welding electrodes is used most commonly. However, for those parts with closed cross sections, it may become necessary to drill a working hole through which the electrodes for direct spot welding of the steel sheets can be passed. In this case, the decline in rigidity of the drilled part being compensated for by using a thicker steel sheet or providing a reinforcing member will inevitably increase the weight of the car body. Therefore, Noma et al. attempted to reduce the steel sheet thickness (weight) and secure the required stiffness simultaneously without drilling any hole in the steel sheets.[15] They studied indirect spot welding, in which the steel sheets are pressed and welded by a couple of electrodes from one side at the same time. Because the steel sheets are pressed by electrodes from one side, the weld sinks and the area of contact between the steel sheets increases (the current density decreases) if an excessive force is applied, making it difficult to perform fusion welding. Conversely, if an excessively large current is applied, the local current density between the electrodes increases because of a shunt current, causing a crack or explosion.

In view of the above problems, the applied pressure was lowered appropriately, the steel sheet was provided with a convex surface so as to limit the conduction passes to the relevant part, and the current density was increased even though the welding current was low. As a result, fusion welding could be performed successfully. However, in the case in which a hydroformed member—a good example of a component with a closed cross section—was applied to the front pillar,[16] the welding conditions, earth electrode position, and welding point sequence were optimized to secure a stable weld quality with the existing equipment. Nippon Steel Corporation, too, tackled the development of indirect spot welding technology for hollow and sheet-formed members. The company studied various welding conditions for the combination of a hollow member with a wall thickness of 1.6 mm and a sheet-formed member with a thickness of 0.7 mm. By using an electrode with a specially designed tip and a DC power supply in combination, we could perform indirect spot welding of the above members without requiring any special pattern of conduction or pressing, even in the presence of a gap between the members or the presence of shunts (existing welding points). An example of the cross section of an indirect spot weld is illustrated in **Fig. 13**, which clearly indicates that a sufficiently large nugget was formed.

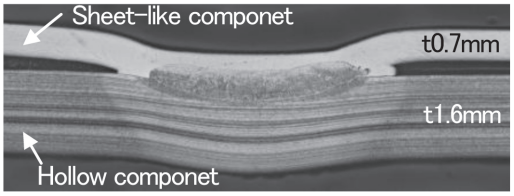

Fig. 13 Cross section of indirect spot weld for hollow and sheet-like components

3. Conclusions

High-strength steels of 980 MPa or more have increasingly been used as materials for the construction of automobiles. At the same time, improvements have been made to the chemical compositions and microstructures of these steels in order to enhance their properties. However, the cross-sectional structures of members and the number and thickness ratio of steel sheets to be welded together have continued to change. Today, therefore, the development of new spot welding techniques suitable for specific conditions is required. In this report, we have discussed current problems in spot welding and their solutions. In the future, we intend to clarify the essence of these problems and propose effective solution technology.

References

1) Okuda, T.: Supottoyousetsu nyumon (An Introduction to Resistance Spot Welding). Sanpo Publications, Inc., 1986
2) Euro Car Body. Data presented by VW. 2008
3) Oikawa, H., Murayama, G., Sakiyama, T., Takahashi, Y., Ishikawa, T.: Shinnittetsu Giho. (385), 36 (2006)
4) Yamazaki, K., Sato, K., Tokunaga, Y.: Quarterly Journal of the Japan Welding Society. 17 (4), 553 (1999)
5) Nishi, T., Saito, T., Yamada, A., Takahashi, Y.: Evaluation of Spot Weldability of High-Strength Sheet Steels for Automobile Use. Nippon Steel Technical Report. (20), 37 (1982)
6) Sakuma, Y., Oikawa, H.: Shinnittetsu Giho. (378), 30 (2003)
7) Watanabe, F., Furusako, S., Hamatani, H., Miyazaki, Y., Nose, T.: Technical Comission on Welded Structure, the Japan Welding Society: Papers for Welded Structure Symposium 2011. 2011, p. 271
8) Miyoshi, T., Shiratori, M.: Transactions of the Japan Society of Mechanical Engineers (Volume A). 47, 424 (1981)
9) Hamatani, H., Watanabe, F., Miyazaki, Y., Tanaka, T., Maki, J., Oikawa, H., Nose, T.: Preprints of the National Meeting of J.W.S, No. 89, 44 (2011)
10) Taniguchi, K., Ikeda, N., Endo, S.: Preprints of the National Meeting of J.W., No. 90, 240 (2012)
11) Watanabe, F., Furusako, S., Miyazaki, Y., Nose, T.: Preprints of the National Meeting of J.W., No. 90, 238 (2012)
12) Sakano, R.: Journal of the Japan Welding Society. 81 (3), 11 (2012)
13) Ikeda, N., Okita, Y., Ono, M., Yasuda, K., Terasaki, T.: Quarterly Journal of the Japan Welding Society. 28 (1), 141 (2010)
14) Takahashi, O.: Pat. No. 4728926
15) Noma, K., Kato, S.: Welding Technology. 110 (2004.1)
16) Hasegawa, Y., Fujita, K., Endo, T., Fujimoto, M., Tanabe, J., Yoshida, M.: Honda R&D Technical Review. 20 (2), 106 (2008.10)

Seiji FURUSAKO
Senior Researcher
Welding & Joining Research Center
Steel Research Laboratories
20-1 Shintomi, Futtsu, Chiba 293-8511

Fuminori WATANABE
Researcher
Welding & Joining Research Center
Steel Research Laboratories

Gen MURAYAMA
Senior Researcher
Welding & Joining Research Center
Steel Research Laboratories

Hideki HAMATANI
Chief Researcher, Dr.Eng.
Nagoya R&D Lab.

Hatsuhiko OIKAWA
Chief Researcher, Dr.Eng.
Welding & Joining Research Center
Steel Research Laboratories

Yasuo TAKAHASHI
Senior Researcher, Dr.Eng.
Welding & Joining Research Center
Steel Research Laboratories

Tetsuro NOSE
General Manager, Dr.Eng.
Welding & Joining Research Center
Steel Research Laboratories